Combined study of the η and η' mesons: phenomenology, chiral extrapolation of lattice QCD and effective field theory [*]

Zhi-Hui Guo[1,2;1]

[1] Department of Physics, Hebei Normal University, Shijiazhuang 050024, China

[2] State Key Laboratory of Theoretical Physics, Institute of Theoretical Physics, CAS, Beijing 100190, China

Abstract: We first carry out a comprehensive phenomenological study of the decay processes with the η or η' in the initial/final states within the effective field theory approach. Two primary types of processes are analyzed: the ones only with light-flavor hadrons and those involving the J/ψ. The couplings from the effective Lagrangian, together with the η-η' mixing parameters from the two-mixing-angle scheme, are fitted to a large number of experimental data, including the various decay widths and the form factors. With the phenomenological mixing parameters and the lattice simulation data of the masses and decay constants of the light pseudoscalar mesons as inputs, we perform a next-to-next-to-leading order study of the η-η' mixing system in $U(3)$ chiral perturbation theory. Updated values of the relevant low energy constants are obtained.

Key words: chiral Lagrangian, η and η' mixing

PACS: 12.39.-x, 13.25.Gv, 13.20.Gd, 11.30.Hv

关于η和η'物理的唯象学和格点手征延拓研究

郭志辉[1,2;1]

[1] 河北师范大学物理科学与信息工程学院，石家庄，050024

[2] 中国科学院理论物理所，理论物理国家重点实验室，北京，100190

摘要： 我们首先在有效场论框架下对η和η'唯象学进行了全面的研究，主要包括两种类型的衰变过程：一种是只含有轻味强子的过程，另一种是有J/ψ参与的反应过程。通过拟合大量相关的衰变宽度和形状因子的实验数据，我们确定了有效拉氏量中自由参数的取值，同时也给出了双混合角机制下的η-η'混合参数。结合通过实验数据定出的混合参数以及格点量子色动力学数值模拟给出的轻赝标介子质量和衰变常数，我们在$U(3)$手征微扰理论框架下对η-η'混合进行了次次领头阶的分析，并给出了更新的低能耦合常数的数值。

关键词： 手征有效场论、η-η'混合

1 Introduction

The light-flavor η and η' mesons provide a valuable window to study many important nonperturbative properties of Quantum Chromodynamics (QCD), including the spontaneously chiral symmetry breaking, the mechanism of explicit breaking of $SU(3)$-flavor symmetry and the $U(1)_A$ anomaly of strong interactions.

There are many experimental collaborations that have measured or planned to measure the physical processes with the η or η' mesons with high precision and high statistics, such as BESIII [1], Jefferson Lab [2], K-LOE [3], CELSIUS/WASA [4], CBELSA/TAPS [5] and CMD-2 [6]. On the other hand, lattice QCD simulations have been greatly progressed on the η and η' mesons and many precise simulation data are released [7–11].

We have performed a thorough analysis on the radiative decay processes involving the η or η' and light-flavor vector resonances within the framework of resonance chiral theory (RχT) in Ref. [12]. In a later work, we extend the discussions to study the decay processes of $J/\psi \to VP, P\gamma^{(*)}$, being V the light-flavor vectors and P the light pseudoscalar mesons [13]. The two-mixing-angle scheme for the η-η' system is used in these phenomenological discussions, and precise values of the four mixing parameters are extracted from the experimental data. Together with the phenomenological determinations of mixing parameters and the lattice simulation data as inputs, we have then carried out the next-to-next-to-leading order (NNLO) study of the η-η' mixing

within the $U(3)$ chiral perturbation theory (χPT). The phenomenological inputs and lattice simulations are successfully reproduced, with reasonable values of low energy constants (LECs) [14]. In this paper, we briefly review the works in Refs. [12–14].

2 Theoretical formalism for the decay processes

2.1 Radiative processes with light-flavor hadrons

To describe the dynamics between the light psuedoscalar mesons and the light-flavor vector resonances, we use the relevant chiral Lagrangian from RχT to calculate the decay widths and form factors. We simply elaborate the pertinent chiral Lagrangians in the following. The kinetic terms for the light vector resonances read

$$\mathscr{L}_{kin}(V) = -\frac{1}{2}\langle \nabla^\lambda V_{\lambda\mu} \nabla_\nu V^{\nu\mu} - \frac{M_V^2}{2} V_{\mu\nu} V^{\mu\nu}\rangle, \quad (1)$$

being $V_{\mu\nu}$ the vector octet plus singlet described in the anti-symmetric tensor formalism [15]. The transitions between the vectors and the photon are governed by the operator [15]

$$\mathscr{L}_2(V) = \frac{F_V}{2\sqrt{2}}\langle V_{\mu\nu} \tilde{f}_+^{\mu\nu}\rangle, \quad (2)$$

where $\tilde{f}_+^{\mu\nu}$ contain the external source fields. We are only interested in the photon field in this work. The VJP operators with one vector field, one external source and one light pseudoscalar, including the singlet η_0 state, read [12, 16]

$$\mathcal{L}_{VJP} = \frac{\tilde{c}_1}{M_V}\varepsilon_{\mu\nu\rho\sigma}\langle\{V^{\mu\nu}, \tilde{f}_+^{\rho\alpha}\}\nabla_\alpha \tilde{u}^\sigma\rangle$$
$$+\frac{\tilde{c}_2}{M_V}\varepsilon_{\mu\nu\rho\sigma}\langle\{V^{\mu\alpha}, \tilde{f}_+^{\rho\sigma}\}\nabla_\alpha \tilde{u}^\nu\rangle + \frac{i\tilde{c}_3}{M_V}\varepsilon_{\mu\nu\rho\sigma}\langle\{V^{\mu\nu}, \tilde{f}_+^{\rho\sigma}\}\tilde{\chi}_-\rangle$$
$$+\frac{i\tilde{c}_4}{M_V}\varepsilon_{\mu\nu\rho\sigma}\langle V^{\mu\nu}[\tilde{f}_-^{\rho\sigma}, \tilde{\chi}_+]\rangle + \frac{\tilde{c}_5}{M_V}\varepsilon_{\mu\nu\rho\sigma}\langle\{\nabla_\alpha V^{\mu\nu}, \tilde{f}_+^{\rho\alpha}\}\tilde{u}^\sigma\rangle$$
$$+\frac{\tilde{c}_6}{M_V}\varepsilon_{\mu\nu\rho\sigma}\langle\{\nabla_\alpha V^{\mu\alpha}, \tilde{f}_+^{\rho\sigma}\}\tilde{u}^\nu\rangle$$
$$+\frac{\tilde{c}_7}{M_V}\varepsilon_{\mu\nu\rho\sigma}\langle\{\nabla^\sigma V^{\mu\nu}, \tilde{f}_+^{\rho\alpha}\}\tilde{u}_\alpha\rangle$$
$$-i\tilde{c}_8 M_V\sqrt{\frac{2}{3}}\varepsilon_{\mu\nu\rho\sigma}\langle V^{\mu\nu}\tilde{f}_+^{\rho\sigma}\rangle\ln(\det\tilde{u}), \quad (3)$$

where the light pseudoscalar multiplet is incorporated in the $\tilde{u}_\mu, \tilde{u}$ and $\chi_\pm$ fields. The VVP types of effective Lagrangian involving η_0 read [12, 16]

$$\mathcal{L}_{VVP} = \tilde{d}_1\varepsilon_{\mu\nu\rho\sigma}\langle\{V^{\mu\nu}, V^{\rho\alpha}\}\nabla_\alpha \tilde{u}^\sigma\rangle$$
$$+i\tilde{d}_2\varepsilon_{\mu\nu\rho\sigma}\langle\{V^{\mu\nu}, V^{\rho\sigma}\}\tilde{\chi}_-\rangle + \tilde{d}_3\varepsilon_{\mu\nu\rho\sigma}\langle\{\nabla_\alpha V^{\mu\nu}, V^{\rho\alpha}\}\tilde{u}^\sigma\rangle$$
$$+\tilde{d}_4\varepsilon_{\mu\nu\rho\sigma}\langle\{\nabla^\sigma V^{\mu\nu}, V^{\rho\alpha}\}\tilde{u}_\alpha\rangle$$
$$-i\tilde{d}_5 M_V^2\sqrt{\frac{2}{3}}\varepsilon_{\mu\nu\rho\sigma}\langle V^{\mu\nu} V^{\rho\sigma}\rangle\ln(\det\tilde{u}). \quad (4)$$

In addition, the relevant part of the Wess-Zumino-Witten Lagrangian is

$$\mathcal{L}_{WZW} = -\frac{\sqrt{2}N_C}{8\pi^2 F}\varepsilon_{\mu\nu\rho\sigma}\langle\Phi\partial^\mu v^\nu\partial^\rho v^\sigma\rangle. \quad (5)$$

We refer to Refs. [12, 15, 16] for further details about the previous Lagrangians. We then calculate the transition amplitudes, depicted by the Feynman diagrams shown in Figs. 1 and 2. With these transition amplitudes, it is straightforward to get the experimentally observed form factors and decay widths [12].

Before ending this section, we elaborate one more detail about the two-mixing-angle scheme to treat the η and η' mesons. The light pseudoscalar octet plus singlet mesons are incorporated in the $\tilde{u}$ field in the previous Lagrangians and we take the following two-mixing-angle formalism when calculating the amplitudes with η or η' states

$$\begin{pmatrix} \eta \\ \eta' \end{pmatrix} = \frac{1}{F}\begin{pmatrix} F_8\cos\theta_8 & -F_0\sin\theta_0 \\ F_8\sin\theta_8 & F_0\cos\theta_0 \end{pmatrix}\begin{pmatrix} \eta_8 \\ \eta_0 \end{pmatrix}, \quad (6)$$

where η_0 and η_8 stand for the $SU(3)$-flavor singlet and octet states, respectively, and η, η' denote the physical states. The four mixing parameters F_0, F_8, θ_0 and θ_8 will be fitted to experimental data.
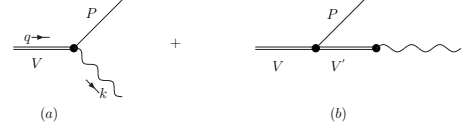

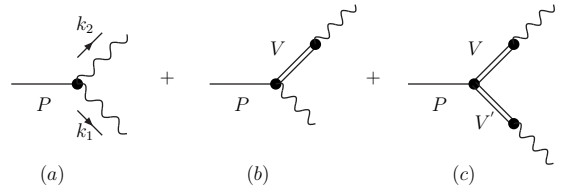Fig. 1. Feynman diagrams for the $VP\gamma^{(*)}$ types of processes.

Fig. 2. Feynman diagrams for the $P\gamma\gamma^{(*)}$ types of processes.

2.2 Calculation of the $J/\psi \to VP, P\gamma^{(*)}$ amplitudes

In this part, we introduce the effective Lagrangian describing the dynamics of the $J/\psi \to VP$ and $P\gamma^{(*)}$ decays. Both the strong and the electromagnetic (EM) interactions will enter into these decays. We include three terms to describe the strong interactions in the $J/\psi \to VP$ decays

$$\mathscr{L}_{\psi VP} = M_\psi h_1 \varepsilon_{\mu\nu\rho\sigma} \psi^\mu \langle \tilde{u}^\nu V^{\rho\sigma} \rangle$$
$$+ \frac{1}{M_\psi} h_2 \varepsilon_{\mu\nu\rho\sigma} \psi^\mu \langle \{\tilde{u}^\nu, V^{\rho\sigma}\} \tilde{\chi}_+ \rangle$$
$$+ M_\psi h_3 \varepsilon_{\mu\nu\rho\sigma} \psi^\mu \langle \tilde{u}^\nu \rangle \langle V^{\rho\sigma} \rangle . \tag{7}$$

Notice that proper M_ψ factors are introduced in the previous equation in order to make the couplings $h_{i=1,2,3}$ dimensionless.

Two effective operators are constructed to describe the $J/\psi P\gamma^{(*)}$ interaction

$$\mathscr{L}_{\psi P\gamma} = g_1 \varepsilon_{\mu\nu\rho\sigma} \psi^\mu \langle \tilde{u}^\nu \tilde{f}_+^{\rho\sigma} \rangle$$
$$+ \frac{1}{M_\psi^2} g_2 \varepsilon_{\mu\nu\rho\sigma} \psi^\mu \langle \{\tilde{u}^\nu, \tilde{f}_+^{\rho\sigma}\} \tilde{\chi}_+ \rangle . \tag{8}$$

The transition strength between the J/ψ and the photon field reads

$$\mathscr{L}_2^\psi = \frac{-1}{2\sqrt{2}} \frac{f_\psi}{M_\psi} \langle \hat{\psi}_{\mu\nu} \tilde{f}_+^{\mu\nu} \rangle , \tag{9}$$

with $\hat{\psi}_{\mu\nu} = \partial_\mu \psi^\nu - \partial_\nu \psi^\mu$.

Together with these effective Lagrangians and also the ones given in Sect. 2.1, we can calculate the $J/\psi \to P\gamma^{(*)}$ and VP amplitudes. The pertinent Feynman diagrams are depicted in Figs. 3 and 4. In order to reasonably reproduce the experimental results of the $J/\psi \to \eta^{(')}\gamma$ decay widths, it is necessary to include the mechanism depicted by the diagram (c) in Fig. 3, i.e. to consider the contribution from the charmonium η_c and also the mixing between η_c and $\eta^{(')}$ [17]. The decay widths and form factors can be easily obtained with the transition amplitudes corresponding to Figs. 3 and 4. We refer to Ref. [13] for further details.
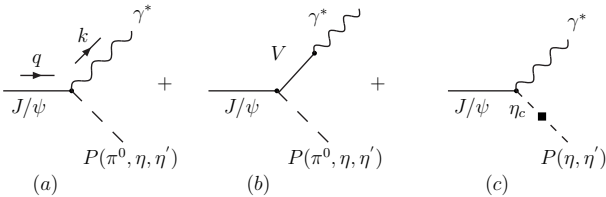

Fig. 3. Relevant Feynman diagrams for the $J/\psi \to P\gamma^*$ decays.
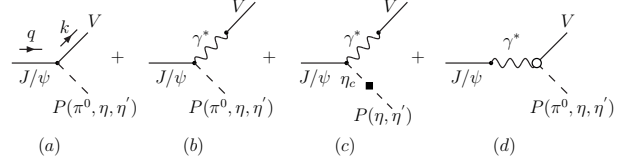

Fig. 4. Relevant Feynman diagrams for the $J/\psi \to VP$ decays.

3 Phenomenological discussions

We consider a large amount of experimental data in our work, including the available decay widths of $P \to V\gamma$, $V \to P\gamma$, $P \to \gamma\gamma$, $P \to \gamma l^+ l^-$, $V \to P l^+ l^-$, $J/\psi \to P\gamma$ and $J/\psi \to VP$ [18], with $P = \pi, K, \eta, \eta'$ and $V = \rho, K^*, \omega, \phi$. In addition, the form factors of $J/\psi \to \eta'\gamma^*$, $\eta \to \gamma\gamma^*$, $\eta' \to \gamma\gamma^*$, $\phi \to \eta\gamma^*$ will be also taken into account. We will make a global fit by including all of these data.

Before presenting our fit results, we point out that with the theoretical formalism in Sect. 2 alone it is impossible for us to reasonably reproduce the $J/\psi \to \omega\pi^0$ decay width. We simply include the excited vector ρ' in this channel to perform the fits [13].

A rather good reproduction of the experimental data in our global fit is achieved, with the $\chi^2/d.o.f$ close to one. The final results for the form factors of $J/\psi \to \eta'\gamma^*$, $\eta \to \gamma\gamma^*$ and $\eta' \to \gamma\gamma^*$ are given in Figs. 5, 6 and 7, respectively. Due to the large experimental error bars, the $\phi \to \eta'\gamma^*$ form factor barely play any important role in the fits and we do not explicitly show the result for this channel [12, 13].

In Table 1, we give the fitted values for the four mixing parameters defined in Eq. (6). In order to highlight the influence of the J/ψ data on the determination of the η-η' mixing, we explicitly show two different fit results. In the global fit, we include all of the previously mentioned experimental data, while in the partial fit situation only the data involving the light-flavor hadrons are taken into account. Although the values of the mixing parameters from the two fits are compatible, the error bars after including the J/ψ data are clearly smaller than those with only the light-flavor data. Therefore one can conclude that the $J/\psi \to VP, P\gamma^{(*)}$ decays are important to constrain the η-η' mixing. For the remaining fitted parameters, we refer to Ref. [13] for details.

Next we analyze the different mechanisms that contribute to the $J/\psi \to P l^+ l^-$ processes. According to the Feynman diagrams in Fig. 3, there are three different kinds of contributions: the contact interacting vertex, the light-vector-resonance exchanges and the η_c-$\eta^{(')}$ mixing. The effects from the intermediate vectors like $J/\psi \to \rho^0 P, \omega P$ and ϕP, with ρ^0, ω and ϕ decaying into the lepton pairs, have been removed when doing experimental analyses for the $J/\psi \to P e^+ e^-$ decays in Ref. [19].

In order to be consistent with the experimental setups, we also drop the diagram (b) in Fig. 3 when fitting to the data. Nevertheless, we point out that it is a priori not justified to neglect the contributions from the intermediate light vectors in the $J/\psi \to Pl^+l^-$ decays. We have made a rough estimate that the light vectors can contribute around 30% in the $J/\psi \to \pi^0 e^+e^-$ decay [13], which qualitatively agrees with the findings in Refs. [27–29]. In our case, large destructive interference between the ρ^0 exchange and other mechanisms in the $J/\psi \to \pi^0\gamma^{(*)}$ are observed. As a result, a larger value of the branching ratio of the $J/\psi \to \pi^0 e^+e^-$ is predicted after neglecting the contributions from the intermediate ρ^0 resonance. So it is meaningful and important to make a revised experimental analyses on the $J/\psi \to \pi^0 e^+e^-$ decays by keeping all of the contributions, instead of removing parts of them. In contrast, the contributions from the intermediate light vectors turn to be negligible in the $J/\psi \to \eta^{(')}\gamma^{(*)}$ decay processes. The branching ratios for the $J/\psi \to Pl^+l^-$ are summarized in Table 2.

Another interesting subject is to analyze the roles of the strong and EM interactions in the $J/\psi \to VP$ decays. In our theoretical formalism, the strong interaction is depicted by the diagram (a) in Fig. 4, while the other diagrams correspond to the EM interactions. We confirm that the EM interactions play the dominant roles in the isospin violated decay channels, such as $J/\psi \to \rho^0\eta^{(')}$, and $\omega\pi^0$, and the strong interactions dominate in the isospin conserved channels, such as $J/\psi \to \rho\pi, \omega\eta^{(')}, \phi\eta^{(')}, K^{*+}K^-$ and $K^{*0}\bar{K}^0$.

Fig. 6. The $\eta \to \gamma\gamma^*$ form factors. The solid (red) line denotes our central values and the shaded areas represent the error bands at one-sigma level. The experimental data are taken from Refs. [20–25]. We clearly show the curve in the timelike region of $s > 0$ in the framed figure.

Fig. 7. The $\eta' \to \gamma\gamma^*$ form factors. The solid (red) line denotes our central results and the shaded areas represent the error bands at one-sigma level. The experimental data are taken from Refs. [22–26].
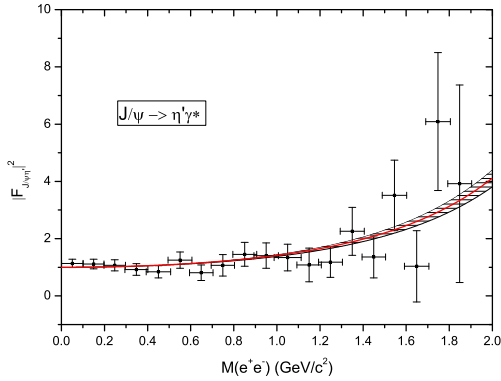

Fig. 5. The $J/\psi \to \eta'\gamma^*$ form factors. The solid (red) line denotes our central results and the shaded areas represent the error bands at one-sigma level. The data are taken from Ref. [19].
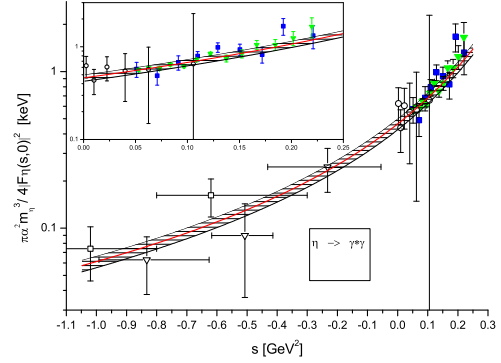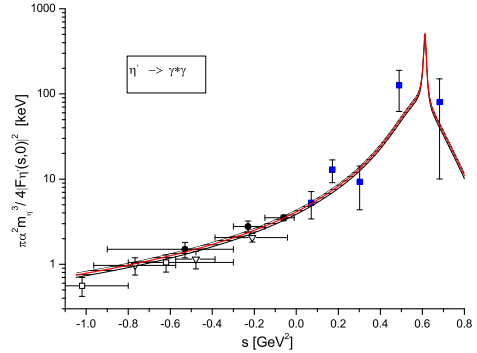
Table 1. Mixing parameters from the fits. See the text for details.

	Global Fit	Partial Fit
F_8 (MeV)	133.7 ± 3.7	126.3 ± 6.5
F_0 (MeV)	118.0 ± 5.5	109.7 ± 16.6
θ_8	$(-26.7 \pm 1.8)°$	$(-21.1 \pm 6.0)°$
θ_0	$(-11.0 \pm 1.0)°$	$(-2.5 \pm 8.2)°$

Table 2. Branching ratios ($\times 10^{-5}$) for the $J/\psi \to Pl^+l^-$ decays.

	Exp	Our results
$\psi \to \pi^0 e^+ e^-$	0.0756 ± 0.0141	0.1191 ± 0.0138
$\psi \to \eta e^+ e^-$	1.16 ± 0.09	1.16 ± 0.08
$\psi \to \eta' e^+ e^-$	5.81 ± 0.35	5.76 ± 0.16
$\psi \to \pi^0 \mu^+ \mu^-$	-	0.0280 ± 0.0032
$\psi \to \eta \mu^+ \mu^-$	-	0.32 ± 0.02
$\psi \to \eta' \mu^+ \mu^-$	-	1.46 ± 0.04

4 Chiral extrapolation of the η and η' masses

Previously when addressing the η-η' mixing, we simply adopt the two-mixing-angle scheme in Eq. (6) and do not give any further explanation to derive the formalism. Next we shall use the $U(3)$ χPT as an underlying theory to calculate the η-η' mixing pattern. In order to establish a consistent power counting, the simultaneous expansions on the momentum squared, light-quark masses and $1/N_C$, which will be denoted as δ expansion, need to be introduced in $U(3)$ χPT. Up to NNLO in δ expansion, the pertinent chiral Lagrangians read

$$\mathcal{L}^{(\delta^0)} = \frac{F^2}{4}\langle u_\mu u^\mu \rangle + \frac{F^2}{4}\langle \chi_+ \rangle + \frac{F^2}{12}M_0^2 X^2, \quad (10)$$

$$\mathcal{L}^{(\delta)} = \quad L_5 \langle u^\mu u_\mu \chi_+ \rangle + \frac{L_8}{2}\langle \chi_+ \chi_+ + \chi_- \chi_- \rangle$$
$$+ \frac{F^2 \Lambda_1}{12}D^\mu X D_\mu X - \frac{F^2 \Lambda_2}{12}X\langle \chi_- \rangle, \quad (11)$$

$$\mathcal{L}^{(\delta^2)} = \frac{F^2 v_2^{(2)}}{4}X^2\langle \chi_+ \rangle + L_4 \langle u^\mu u_\mu \rangle \langle \chi_+ \rangle + L_6 \langle \chi_+ \rangle \langle \chi_+ \rangle$$
$$+ L_7 \langle \chi_- \rangle \langle \chi_- \rangle + L_{18}\langle u_\mu \rangle \langle u^\mu \chi_+ \rangle + L_{25}X\langle \chi_+ \chi_- \rangle$$
$$+ C_{12}\langle h_{\mu\nu}h^{\mu\nu}\chi_+ \rangle + C_{14}\langle u_\mu u^\mu \chi_+ \chi_+ \rangle + C_{17}\langle u_\mu \chi_+ u^\mu \chi_+ \rangle$$
$$+ C_{19}\langle \chi_+ \chi_+ \chi_+ \rangle + C_{31}\langle \chi_- \chi_- \chi_+ \rangle. \quad (12)$$

With these chiral Lagrangians, one can then calculate the η-η' mixing pattern and express the mixing parameters in Eq. (6) in terms of the chiral LECs in Eqs. (10), (11) and (12). Due to the lengthy formulas, we refer to Ref. [14] for further details about the relations between the mixing parameters and LECs.

One of the biggest challenges when calculating the η-η' mixing pattern in $U(3)$ χPT is to determine the many unknown LECs. The precise lattice simulations of the light pseudoscalar mesons are valuable to constrain the values of the unknown LECs. We shall include in our fits the m_π dependence of the η and η' masses [7–11], the kaon masses [30, 31], the π, K decay constants [30, 31] and their ratios [32]. The previously determined phenomenological results of the η-η' mixing parameters shall be also used to constrain these LECs.

It is interesting to mention that even at leading order the $U(3)$ χPT, which only has one free parameter,

can reasonably reproduce the lattice simulation data, as shown in Fig. 8. While in order to simultaneously describe the lattice simulations on the light pseudoscalar mesons, specially the pion and kaon decay constants, it is essential to include the NNLO contributions. Among the NNLO LECs in Eq. (12), we fix $v_2^{(2)}, L_{18}, L_{25}$ to zero, due to their marginal effects in our present discussion. While for the poorly known $\mathcal{O}(p^6)$ LECs C_i, we multiply the values of C_i from Refs. [33, 34] by a common factor α in our fits. We find that two different sets of values from Refs. [33, 34] lead to more or less similar results. Therefore, we only present the NNLO fit results by taking the values of C_i from Ref. [34] in Table 3. The values obtained here are compatible with the recent two-loop determinations of the next-to-leading order LECs [35]. The NNLO reproduction of the lattice simulation data is quite successful [14] and therefore the $U(3)$ chiral perturbation theory can be considered as a useful tool to perform the chiral extrapolation of the lattice data for the light pseudoscalars.
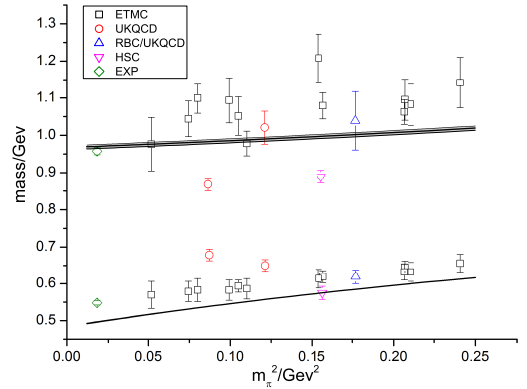

Fig. 8. The LO fit of the η and η' masses. The lattice simulation data are from Refs. [7–11].

Table 3. The values of the parameters from the NNLO fits by taking the $\mathcal{O}(p^6)$ LECs from Ref. [34].

F (MeV)	$81.7 \pm 1.5 \pm 5.3$
$10^3 \times L_5$	$0.60 \pm 0.11 \pm 0.52$
$10^3 \times L_8$	$0.25 \pm 0.07 \pm 0.31$
Λ_1	$-0.003 \pm 0.060 \pm 0.093$
Λ_2	$0.08 \pm 0.11 \pm 0.20$
$10^3 \times L_4$	$-0.12 \pm 0.06 \pm 0.19$
$10^3 \times L_6$	$-0.05 \pm 0.04 \pm 0.02$
$10^3 \times L_7$	$0.26 \pm 0.05 \pm 0.06$
α	$-0.59 \pm 0.09 \pm 0.18$

5   Conclusions

Within the effective Lagrangian approach, we have made a comprehensive study of the processes involving η or η' mesons, including the radiative decays with light-flavor hadrons, such as the types of $VP\gamma^{(*)}$, $P\gamma\gamma^{(*)}$, and also the $J/\psi \to P\gamma^{(*)}$ and VP decays, being $P = \pi, K, \eta, \eta'$ and $V = \rho, K^*, \omega, \phi$. The modern recipe of the two-mixing-angle scheme is used to describe the η and η' mesons. We make a global fit by considering a large amount of the experimental data. Reliable values of the η-η' mixing parameters, together with the resonance couplings from the effective Lagrangian, are determined. We point out that the contributions from the intermediate light vectors in the $J/\psi \to \pi^0\gamma$ and $J/\psi \to \pi^0 l^+l^-$ decays, with $l = e, \mu$, are important. Therefore a future revised experimental measurement is crucial to verify this mechanism.

We further calculate the η-η' mixing pattern from the underlying $U(3)$ chiral perturbation theory. And the four mixing parameters are expressed in terms of the chiral low energy constants. By including the lattice simulation data of the masses of η, η' and kaon, and the pion and kaon decay constants, we carry out a next-to-next-to-leading order study and determine the relevant chiral low energy constants, which are consisten with the recent two-loop results. We conclude that the $U(3)$ chiral perturbation theory can provide a useful tool to perform the chiral extrapolations of the lattice QCD data for the light pseudoscalar mesons.

References

1 H. B. Li, "eta and eta-prime Physics at BES-III," J. Phys. G, 2009, **36**: 085009; Z. Y. Zhang, L. Q. Qin and S. S. Fang, "Event generators for eta/eta-prime rare decays into pi+ pi- l+ l- and e+ e- mu+ mu-," Chin. Phys. C, 2012 **36**: 926; S. S. Fang [BESIII Collaboration], "Eta and eta' Physics at BESIII," PoS CD **12**, 2013: 036 .

2 L. P. Gan and A. Gasparian, "Search of new physics via eta rare decays," PoS CD **09**, 2009: 048.

3 G. Amelino-Camelia *et al.*, "Physics with the KLOE-2 experiment at the upgraded DAϕNE," Eur. Phys. J. C, 2010, **68**: 619 .

4 M. Berlowski *et al.* [CELSIUS/WASA Collaboration], "Measurement of eta meson decays into lepton-antilepton pairs," Phys. Rev. D, 2008, **77**: 032004 .

5 V. Crede *et al.* [CBELSA/TAPS Collaboration], "Photoproduction of eta and eta-prime mesons off protons," Phys. Rev. C, 2009, **80**: 055202 .

6 R. R. Akhmetshin *et al.* [CMD-2 Collaboration], "Study of conversion decays $\phi \to \eta e^+e^-$, $\eta \to e^+e^-\gamma$ and $\eta \to \pi^+\pi^-e^+e^-$ at CMD-2," Phys. Lett. B, 2001, **501**: 191.

7 J. J. Dudek, R. G. Edwards, B. Joo, M. J. Peardon, D. G. Richards and C. E. Thomas, "Isoscalar meson spectroscopy from lattice QCD," Phys. Rev. D, 2011, **83**: 111502.

8 N. H. Christ, C. Dawson, T. Izubuchi, C. Jung, Q. Liu, R. D. Mawhinney, C. T. Sachrajda and A. Soni *et al.*, "The η and η' mesons from Lattice QCD," Phys. Rev. Lett. 2010, **105**: 241601 .

9 E. B. Gregory *et al.* [UKQCD Collaboration], "A study of the eta and eta' mesons with improved staggered fermions," Phys. Rev. D, 2012, **86**: 014504 .

10 C. Michael *et al.* [European Twisted Mass Collaboration], "η and η' masses and decay constants from lattice QCD with $N_f = 2 + 1 + 1$ quark flavours," PoS LATTICE **2013**, 2014: 253.

11 C. Michael *et al.* [ETM Collaboration], "η and η' mixing from Lattice QCD," Phys. Rev. Lett. 2013, **111**, no. 18: 181602 .

12 Y. H. Chen, Z. H. Guo and H. Q. Zheng, "Study of η-η' mixing from radiative decay processes," Phys. Rev. D, 2012, **85**: 054018 .

13 Y. H. Chen, Z. H. Guo and B. S. Zou, "Unified study of $J/\psi \to PV$, $P\gamma^{(*)}$ and light hadron radiative processes," Phys. Rev. D, 2015, **91**: 014010.

14 X. K. Guo, Z. H. Guo, J. A. Oller and J. J. Sanz-Cillero, "Scrutinizing the η-η' mixing, masses and pseudoscalar decay constants in the framework of U(3) chiral effective field theory," JHEP, 2015, **1506**: 175 .

15 G. Ecker, *et al.*, "The Role of Resonances in Chiral Perturbation Theory," Nucl. Phys. B, 1989, **321**: 311.

16 P. D. Ruiz-Femenia, A. Pich and J. Portoles, "Odd intrinsic parity processes within the resonance effective theory of QCD," JHEP, 2003, **0307**: 003.

17 K. T. Chao, "Mixing of eta, eta-prime with c anti-c, b anti-b states and their radiative decays," Nucl. Phys. B, 1990, **335**: 101.

18 K. A. Olive *et al.* [Particle Data Group Collaboration], "Review of Particle Physics," Chin. Phys. C, 2014, **38**, 090001.

19 M. Ablikim *et al.* [BESIII Collaboration], "Observation of electromagnetic Dalitz decays $J/\psi \to Pe^+e^-$," Phys. Rev. D, 2014, **89**, no. 9: 092008.

20 R. Arnaldi *et al.* [NA60 Collaboration], "Study of the electromagnetic transition form-factors in $\eta \to \mu^+\mu^-\gamma$ and $\omega \to \mu^+\mu^-\pi^0$ decays with NA60," Phys. Lett. B, 2009, **677**: 260.

21 M. N. Achasov *et al.*, "Study of Conversion Decays $\phi \to \eta e^+e^-$ and $\eta \to \gamma e^+e^-$ in the Experiment with SND Detector at the VEPP-2M Collider," Phys. Lett. B, 2001, **504**: 275.

22 R. I. Dzhelyadin *et al.*, "Investigation of η Meson Electromagnetic Structure in $\eta \to \mu^+\mu^-\gamma$ Decay," Phys. Lett. B, 1980, **94**: 548.

23 R. I. Dzhelyadin *et al.*, "Observation of $\eta' \to \mu^+\mu^-\gamma$ Decay," Phys. Lett. B, 1979, **88**: 379 .

24 H. Aihara *et al.* [TPC/Two Gamma Collaboration], "Investigation of the electromagnetic structure of η and η' mesons by two photon interactions," Phys. Rev. Lett., 1990, **64**: 172.

25 H. J. Behrend *et al.* [CELLO Collaboration], "A Measurement of the pi0, eta and eta-prime electromagnetic form-factors," Z. Phys. C, 1991, **49**: 401.

26 M. Acciarri *et al.* [L3 Collaboration], "Measurement of eta-prime (958) formation in two photon collisions at LEP-1," Phys. Lett. B, 1998, **418**: 399.

27 B. Kubis and F. Niecknig, "Analysis of the $J/\psi \to \pi^0\gamma^*$ transition form factor," Phys. Rev. D, 2015, **91**, no. 3: 036004.

28 J. L. Rosner, "Meson-Photon Transition Form Factors in the Charmonium Energy Range," Phys. Rev. D, 2009, **79**: 097301.

29 Q. Zhao, "Understanding the radiative decays of vector charmonia to light pseudoscalar mesons," Phys. Lett. B, 2011, **697**, 52.

30 Y. Aoki *et al.* [RBC and UKQCD Collaborations], "Continuum Limit Physics from 2+1 Flavor Domain Wall QCD," Phys. Rev. D, 2011, **83**: 074508.

31 R. Arthur *et al.* [RBC and UKQCD Collaborations], "Domain Wall QCD with Near-Physical Pions," Phys. Rev. D, 2013, **87**: 094514.

32 S. Durr *et al.*, "The ratio FK/Fpi in QCD," Phys. Rev. D, 2010, **81**,054507.

33 S. Z. Jiang, *et al.*, "Computation of the p**6 order chiral Lagrangian coefficients," Phys. Rev. D, 2010, **81**: 014001.

34 S. Z. Jiang, *et al.*, "Computation of the $O(p^6)$ order low-energy constants: An update," Phys. Rev. D, 2015, **92**: 025014.

35 J. Bijnens and G. Ecker, "Mesonic low-energy constants," Ann. Rev. Nucl. Part. Sci., 2014, **64**: 149.